Sensitivity of global climate to the detrimental impact of smoke on rain clouds

Hans-F. Graf[1], Daniel Rosenfeld[2] and Frank J. Nober[1]

1: Max Planck Institute for Meteorology, Hamburg, Germany.
2: Institute of Earth Sciences, The Hebrew University of Jerusalem, Israel.

January 2001

ISSN 0937-1060

Abstract.
The recently reported detrimental impact of air pollution on rainfall at the cloud scale [Rosenfeld et al., 1998] raises the question of its possible impacts at the regional and global scales. The sensitivity of the global atmospheric circulation to air pollution was investigated by assessing the impact of biomass burning on convective rainfall, using a global circulation model [Roeckner et al., 1992]. In spite of conservative assumptions, large sensitivity of the climate system was observed. A possible link between the smoke from biomass burning and the El Niño was identified. Aerosols suppress precipitation from deep tropical clouds and modify the upper tropospheric and stratospheric thermal structure, which induces changes in the global circulation and storm tracks. The simulated changes are in agreement with significant trends observed in tropospheric and stratospheric circulation over the last 50 years.

1 Introduction

About 70 % of the solar energy reaching the earth surface is consumed by the evaporation of water. When the inverse process occurs - condensation into liquid water that returns to the earth's surface as precipitation - latent heat is converted to sensible heat, which induces density and pressure gradients that propel the global atmospheric circulation. Therefore, any changes in precipitation, especially in the tropics, induce major changes in the global climate patterns. The ENSO cycle is an example of such process.

This report deals with the yet little recognized mechanism for changing the climate system in response to anthropogenically induced changes in the precipitation. Recent observations [Rosenfeld et al., 1998, Rosenfeld, 1999, Rosenfeld, 2000] show the detrimental effects of smoke produced by biomass burning and other sources on the efficiency of water and ice precipitation associated with convective clouds. The resulting excess water vapor remaining in the atmosphere eventually precipitates elsewhere. This redistribution of the large scale precipitation and latent heating generates alterations in the driving force behind atmospheric circulations. Hence, the question arises whether microphysical processes can influence large scale dynamics or even global climate. Here we address this question using a state-of-the-art climate model [Roeckner et al., 1992].

Considerable effort has been made in the recent past to estimate the effect of anthropogenically augmented aerosols (mainly sulfate) on the optical properties and on the lifetimes of shallow clouds. The overall effect, as proposed by these studies, is to partly counteract warming produced by "greenhouse gases" [Lohmann et al., 1997]. Although microphysical and optical properties of shallow (depth up to 1.5 km) clouds are treated quite well in the most recent models [Lohmann et al., 1997, Roelofs et al., 1998] nearly no attempt has been made to assess the corresponding effects of convective clouds. Such effect needs to be considered because it is primarily the net energy released by the water condensation vapor and condensate fallout in these specific clouds that drives the atmospheric circulation.

The tropics and subtropics deserve special attention, because most of the global precipitation occurs there. In addition, these regions are prone to increasing amounts of smoke from biomass burning, associated with rapid deforestation. Over the last 30 years, the burned area in which the tropical rainforest has been typically more than 20 million hectares per year [Hao et al., 1990]. The massive population increase in large parts of Southeast Asia, Africa and South America has added to the commercially driven biomass burning activity. Crutzen and Andreae [Crutzen et al., 1990] estimate the gross production of primary aerosols formed from particulate carbon, elemental carbon and potassium to sum up to 36 to 154 Tg per year from biomass burning alone. In addition, 2.1 to 5.5 Tg of NOx -N and 1 to 4 Tg of sulfur are believed to produce secondary aerosol from biomass burning.

New satellite observations clearly demonstrate that aerosols generated by burning vegetation [Rosenfeld et al., 1998, Rosenfeld, 1999], urban and industrial air pollution [Rosenfeld, 2000] suppress the precipitation forming processes in convective clouds.

Many of the aerosol particles act as cloud condensation nuclei (CCN) that form a large number of small cloud droplets. The smaller the droplets are the slower they coalesce into raindrops [Squires, 1958], and also the slower they freeze and form precipitation through the ice processes [Pruppacher et al., 1997]. This finding is supported by aircraft observations [Rosenfeld et al., 2000]. These observations show that, under conditions of weak coalescence, ice precipitation processes are also suppressed, and much of the cloud water is evicted into the upper troposphere through their tops. [Graf et al., 1979] found a reduction of precipitation by 10fresh maritime air masses. Roberts et al. (submitted to Science August 2000) have highlighted the particular role of the Amazon region. They found a very small number of cloud condensation nuclei over the rainforest, suggesting that clouds there have primarily a maritime character. Only under the influence of smoke from biomass burning or industrial emissions, well developed non-precipitating clouds were found. Due to the small background concentration of CCN, this remote area is probably highly sensitive to anthropogenic disturbances. These observations support model results, which quantify the effect. [Reisin et al., 1996] simulated rainfall amounts from convective clouds typical to those producing most of the rainfall in Israel, with tops near -20 ^{0}C. When changing only the CCN spectra from those typical of maritime to polluted continental regimes, the rainfall amount was reduced to only 14 % of that from clouds in the clean air masses.

The detection and attribution of the impact of smoke on precipitation at scales larger than individual clouds requires a much improved treatment of convective clouds and of their microphysics in climate models. In this paper, we address the sensitivity of these processes and present first results provided by a global circulation model that includes the effect of smoke from biomass burning on the formation of convective rain.

2 Model and experiment

For the simulation experiment we used the ECHAM4 atmospheric model at T30 resolution (time step 30 minutes). The formation of precipitation in convective clouds is treated by an extremely simple parameterization. Convective precipitation forms if the cloud extends vertically over a layer covering a depth of at least 150 hPa. When this condition is met, the formation of precipitation depends linearly on the liquid water mixing ratio, with an empirical proportionality factor.

To be consistent with observations, a temperature dependency to this factor was introduced by reducing the formation of new precipitation to 75% for $T > 265$ K [Rosenfeld et al., 1998, Rosenfeld, 1999, Rosenfeld, 2000]. Since little is known regarding the impact on the ice processes, no effect was assumed to occur at $T < 263$ K. The vertical profile of the factor is taken from observations [Rosenfeld, 1999, Rosenfeld, 2000] and we implicitly assume that about 25% of the convective clouds in a grid box are affected by the smoke. This conservative parameterization is applied only at grid points where the emission rate from biomass burning exceeds a critical value. In the extreme case this formulation leads to a reduction of warm (i.e. excluding the freezing process) precipitation formation of about 25%. The critical emission value (8.6 g/m^2 black carbon per day) is based on monthly emission data [Cooke and Wilson]. We assume that above this threshold, smoke plumes are dense enough to influence the microphysical processes of a considerable fraction of the convective clouds. This conservative assumption was tested in a more complex model simulation with interactive aerosols and clouds (Graf, in preparation). With the above critical emission, biomass burning seasons can be well separated for the main regions. There is a need for more intensive studies to better constrain this figure. A 15 year control simulation was performed and followed by the experimental run simulating the effect of the smoke. Such a simulation provides a large enough statistical ensemble to investigate standard and non-standard physical quantities like convective heating rates. A simple statistical significance test normalizing the anomalies (isolines in the Figures) to the local standard deviation (SDV) (shaded areas in the Figures) was applied.

3 Results

We are aware of the simplicity of our approach. We point out, however, that this first numerical experiment provides only a sensitivity study to assess the strength of the effect without making major changes in the existing convective parameterization. Therefore, rather than discussing detailed results of the simulations, we will concentrate on a few major aspects of the global circulation and the climate as first-order indicators of their sensitivity to the biomass burning pollution. The most interesting and potentially important features are pershaps found in the boreal regions during late winter. As mentioned above, convective precipitation is a first order process in the energy cycle of the atmosphere, and, in addition to local and regional effects, global scale changes, which represent feedbacks in the dynamical system are also found.

The lack of a clear annual effect in the regions where large amounts of biomass are burned (i.e. Africa, South America, Indonesia) is caused by the out of phase behavior of rain and fire. This means that the most fires happen during the dry seasons. Convective precipitation dominates in the tropics, where the biomass burning is concentrated. In the zonal mean, convective precipitation shifts with the annual course of the sun and its maximum represented by the Intertropical Convergence Zone, ITCZ over the continents is always found in the summer hemisphere. Over much of the oceans, however, it is always located in the northern hemisphere. In the global average, there is very little change in precipitation amount (Table 1) when the smoke effect is considered. Except in Indonesia, where the most intense convective rainfall takes place, a fraction of the precipitation deficit is balanced by some increase in the large-scale rainfall. There is only a very small net effect on the global mean radiation budget (reduction of solar and gain of terrestrial radiation remaining below 0.1 W/m^2). Together with the changes in rainfall we find altered convective heating rates.

Large scale changes in convective activity also have an influence on the velocity potential (VP), which has its strongest negative values (rising motion) over the Western

Pacific. The meridional position of this activity center follows the sun as well. Consideration of the effect of smoke leads to changes in the VP of the order of 10%, mainly in the upper troposphere. As an example, the center of negative VP (isolines in Figure 1) in March is clearly shifted towards the central Pacific due to positive anomalies over Indonesia and negative ones over the central Pacific. This has important consequences for the wind stress at the surface of the Pacific Ocean, where the easterly stress is reduced significantly (Figure 2). This is especially important since at this time of the year westerly wind anomalies may result in oceanic Kelvin waves which are believed to generate El Niño events [Philander, 1989]. Hence, a positive feedback is suggestive between El Niño, which is responsible for dryness over Indonesia (i.e. for good burning conditions, and the smoke effect that reduces the easterlies near the equator. In our model simulation the SST was held fixed at climatological values. Therefore, such feedbacks were not investigated.

During November and December cloudiness in the middle and upper troposphere is clearly enhanced due to smoke effect on convective clouds at low latitudes and we find a significant warming in the upper troposphere (e. g. of the layer depth 200 hPa - 400 hPa, not shown here). Adiabatic lifting then results in a cooling of the stratosphere (Figure 3). Beginning in January, reduced latent heat release in the tropical upper troposphere leads to cooling, which is strongest close to the tropopause. As a direct response, large scale sinking of stratospheric air produces adiabatic warming in the tropical stratosphere, which is strongest during northern late winter (Figure 3). The low latitude thermal forcing in a positive feedback loop results in a stronger and colder stratospheric polar vortex (SPV) over the Northern Hemisphere in late boreal winter (Figure 4). The leading fundamental coupled variability mode for tropospheric and stratospheric circulation [Perlwitz et al., 1995] is enhanced and leads to stratospheric and tropospheric circulation and to climate anomalies of the type that are well known to occur after tropical volcanic eruptions [Graf et al., 1993]. Such anomalies were shown to be also caused by the rising greenhouse gas concentrations in the atmosphere and ozone destruction [Graf et al, 1998, Shindel et al. 1998]. As shown by Figure 5, the same typical warming in the lower troposphere over mid to high latitude northern continents can be caused during the late winter by the influence of smoke on precipitation. Furthermore, these changes are associated with geopotential height anomalies at 500 hPa (not shown), among other things, indicating a strengthening of the Icelandic low and the Azores high. This leads to a positive North Atlantic Oscillation (NAO) index in the latter half of the winter. A reduced NAO in the early winter due to adiabatic cooling of the low latitude lower stratosphere is also found (not shown here).

The thermal forcing of the SPV induced by aerosols is superimposed on the effects of enhanced SPV due to other causes, such as increased greenhouse gases and ozone destruction [Graf et al, 1998, Shindel et al. 1998]. These effects may work in opposite directions in the early winter, and in the same direction in late winter, resulting in near zero effects in the early winter and a very strong enhancement of the SPV and NAO in the late winter (see Figure 3).

In summary, a very simple and conservative parameterization of the observed impact of aerosols on the convective rainfall, introduced in a global circulation model, leads to significant perturbations of the general circulation at regional and global scales. The microphysical effects of smoke indirectly lead to global scale changes in the tropical Walker and Hadley circulations, in the intensitiy of the boreal winter polar vortex and in midlatitude climate. Possible links between the aerosols and El Niño and NAO were also identified. Although the present study should be regarded as preliminary, it is already clear that the impact of cloud-aerosol interactions on precipitation processes should be considered as a major anthropogenic factor affecting the climate system.

Figure captions

Figure 1: Velocity potential 200 hPa level minus 900 hPa level (isolines) $[m^2/s * 10^{-5}]$ in March (positive values indicate large scale sinking motion) and anomalies due to the effect of smoke on convective precipitation (colored areas).

Figure 2: Wind stress in Pa (isolines) over the western and central Pacific in March and anomalies due to the effect of smoke on convective precipitation (colored areas).

Figure 3: The annual march of the 50 hPa zonally averaged temperature anomaly in K (isolines) due to the effect of smoke on convective precipitation. Shading indicates normalization to standard deviation (SDV).

Figure 4: Vertical distribution of the zonal mean temperature anomaly [K] in March, Isolines for absolute values, shading indicates normalization to SDV.

Figure 5: Lower troposphere (850 hPa) temperature anomaly [K] in March, Northern Hemisphere. Isolines for absolute values, shading indicates normalization to SDV.

Literatur

[Cooke and Wilson] Cooke and Wilson, http://blueskies.sprl.umich.edu/geia/

[Crutzen et al., 1990] Crutzen, P. J. and M. O. Andreae, Biomass burning in the tropics: Impact on atmospheric chemistry and biogeochemical cycles, *Science, 250*, 1669-1678, 1990.

[Graf et al., 1979] Graf, H.-F. and I. Gräfe, Precipitation distribution in the Berlin area depending on height weather and surface wind direction, *Z. Meteor. 29*, 56-64, 1979 (German).

[Graf et al., 1993] Graf, H.-F.; I. Kirchner; A. Robock and I. Schult, Pinatubo eruption winter climate effects: Model versus observation, *Climate Dyn. 9*, 81-93, 1993.

[Graf et al, 1998] Graf, H.-F., I. Kirchner, and J. Perlwitz, Changing stratospheric circulation: The role of ozone and greenhouse gases, *J. Geophys. Res., 103*, 11.251-11.261, 1998.

[Hao et al., 1990] Hao, W. M., M. H. Liu, P. J. Couton, in: Fire in the tropical biota. Ecological studies, vo. 84, J. G. Goldammer, Ed. (Springer Verlag Berlin, 1990) pp. 440-462.

[Lohmann et al., 1997] Lohmann, U., J. Feichter, Impact of sulfate aerosols on albedo and lifetime of clouds, *J. Geophys. Res. 102*, 13685-13700, 1997.

[Perlwitz et al., 1995] Perlwitz, J. and H.-F. Graf, The statistical connection between tropospheric and stratospheric circulation of the Northern hemisphere in winter, J. of Clim., 10, 2281-2295, 1995.

[Philander, 1989] Philander, S. G.: El Niño, La Niña, and the Southern oscillation. Intl. Geophysics Series No. 46, Academic Press, San Diego, 1989, 289 pp.

[Pruppacher et al., 1997] Pruppacher, H. R. and J. D. Klett, Microphysics of clouds and precipitation, Kluwer Academic Publishers, 2nd edn., 1997.

[Reisin et al., 1996] Reisin, T., S. Tzivion, and Z. Levin, Seeding convective clouds with ice nuclei or hygroscopic particles: a numerical study using a model with detailed microphysics. *J. Appl. Meteor., 35*, 1416-1434, 1996.

[Roeckner et al., 1992] Roeckner, E. et al., Simulation of the present day climate with the ECHAM model: Impact of model physics and resolution, Rep. 93, Max Planck Institute for Meteorology, Hamburg, Germany, 1992.

[Roelofs et al., 1998] Roelofs, G. J., J. Lelieveld and L. Ganzeveld, Simulation of global sulfate distribution and the influence of effective cloud drop radii with a coupled photochemistry-sulfur cycle model, *Tellus, 50B*, 224-242, 1998.

[Rosenfeld et al., 1998] Rosenfeld, D., M. I. Lensky, Satellite-Based insights into precipitation formation processes in continental and maritime convective clouds, *Bull. Am. Meteorol. Soc.*, 2457-2476, 1998.

[Rosenfeld, 1999] Rosenfeld, D., TRMM observed first direct evidence of smoke from forest fires inhibiting rainfall, *Geophys. Res. Let. 20*, 3105-3108, 1999.

[Rosenfeld, 2000] Rosenfeld D., Suppression of Rain and Snow by Urban and Industrial Air Pollution. *Science, 287 (5459)*, 1793-1796, 2000.

[Rosenfeld et al., 2000] Rosenfeld D. and W. L. Woodley: Convective Clouds with Sustained Highly Supercooled Liquid Water Down to -37.5oC. *Nature, 405*, 440-442, 2000.

[Shindel et al. 1998] Shindell, Drew T., D. Rind, and P. Lonergan, Increased polar stratospheric ozone losses and delayed eventual recovery owing to increasing greenhouse-gas concentrations, *Nature, 392*, 589-592,1998.

[Squires, 1958] Squires, P., 1958: The microstructure and colloidal stability of warm clouds. *Tellus 10*, 256-271.

Tables

Table 1.
Change (in %) of precipitation due to smoke from biomass burning during the burning season

Area	convective	total
Indonesia	-0.4	-1.2
North Africa ($> 5^0 N$)	-6.8	-6.8
South Africa ($< 5^0 N$)	-2.0	-0.7
South America	-8.0	-5.1
global	-0.4	-0.06

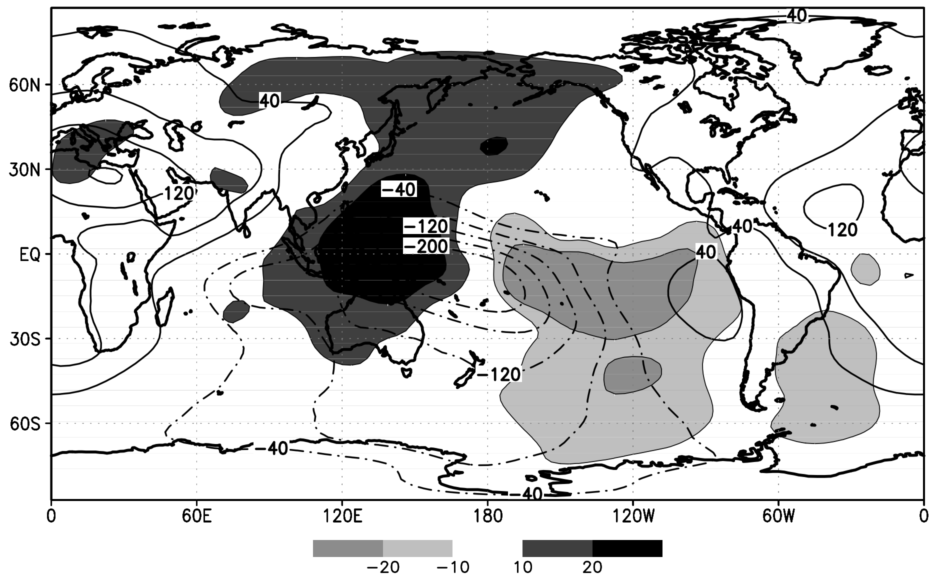

Figure 1: *Velocity potential 200 hPa level minus 900 hPa level (isolines)* $[m^2/s*10^{-5}]$ *in March (positive values indicate large scale sinking motion) and anomalies due to the effect of smoke on convective precipitation (colored areas).*

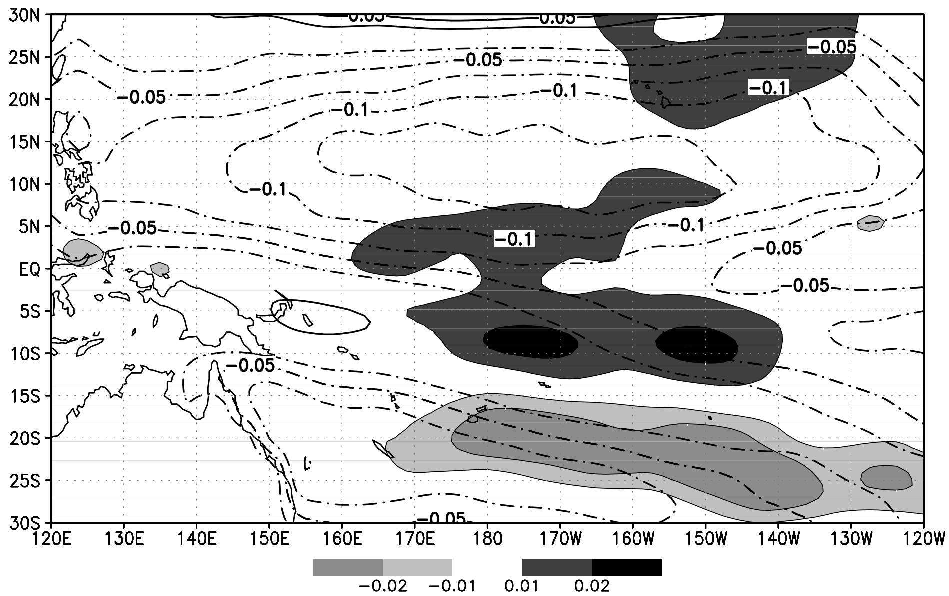

Figure 2: *Wind stress in Pa (isolines) over the western and central Pacific in March and anomalies due to the effect of smoke on convective precipitation (colored areas).*

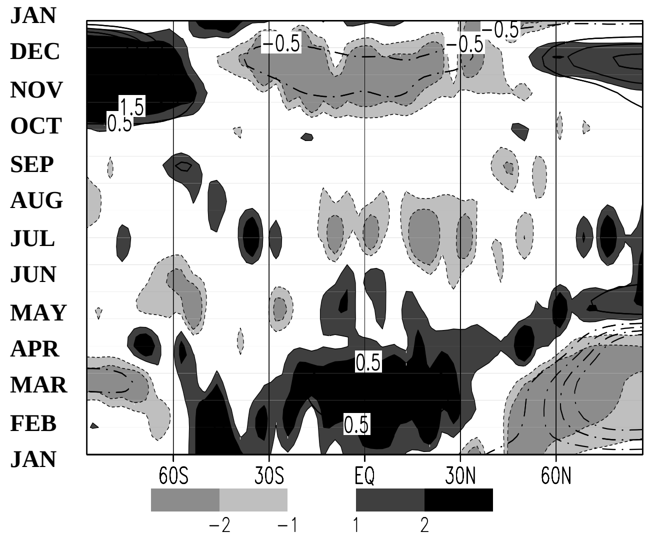

Figure 3: *The annual march of the 50 hPa zonally averaged temperature anomaly in K (isolines) due to the effect of smoke on convective precipitation. Shading indicates normalization to standard deviation (SDV).*

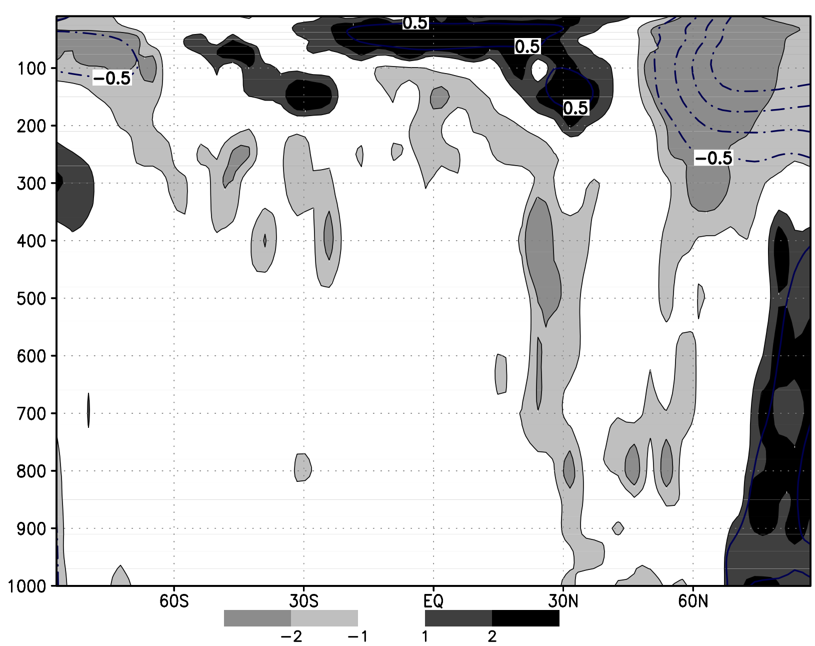

Figure 4: *Vertical distribution of the zonal mean temperature anomaly [K] in March, Isolines for absolute values, shading indicates normalization to SDV.*

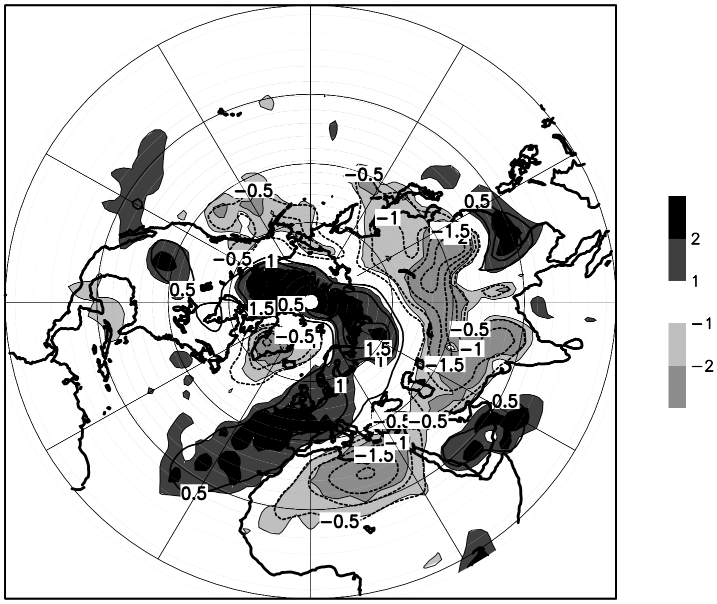

Figure 5: *Lower troposphere (850 hPa) temperature anomaly [K] in March, Northern Hemisphere. Isolines for absolute values, shading indicates normalization to SDV.*